Journal of Molecular Liquids 222 (2016) 398–406

Contents lists available at ScienceDirect

Journal of Molecular Liquids

journal homepage: www.elsevier.com/locate/molliq

Binding of 6-methyl-3-phenyliminomethyl-4H-chromen-4-one with bovine serum albumin in free and β-cyclodextrin-complexed forms: Modulation of the binding by β-cyclodextrin

Sowrirajan Chandrasekaran [a], Natesan Sudha [a], Dhanaraj Premnath [b], Israel V.M.V. Enoch [a,*]

[a] Nanotoxicology Research Lab, Department of Science and Humanities, Karunya University, Coimbatore 641 114, Tamil Nadu, India
[b] Department of Biosciences & Technology, Karunya University, Coimbatore 641 114, Tamil Nadu, India

ARTICLE INFO

Article history:
Received 17 January 2016
Received in revised form 13 July 2016
Accepted 15 July 2016
Available online 19 July 2016

Keywords:
Schiff's base
β-cyclodextrin
bovine serum albumin
fluorescence spectroscopy
ROESY

ABSTRACT

We report in this paper that β-cyclodextrin modulates the binding of a Schiff's base derivative, 6-methyl-3-phenyliminomethyl-4H-chromen-4-one, with the protein bovine serum albumin. The stoichiometry, the association constant, and the mode of association of the derivative with β-cyclodextrin are investigated by ultraviolet-visible absorption, steady-state and time-resolved fluorescence, and proton nuclear magnetic resonance and two dimensional correlation spectroscopic techniques. The structure of the host–guest complex is proposed. The binding of the chromen-4-one with bovine serum albumin and the influence of the added β-cyclodextrin on the binding are reported. β-cyclodextrin is found to decrease the Stern–Volmer quenching constant and the binding strength of the compound with the protein. The donor-to-acceptor distance is altered by the addition of β-cyclodextrin as studied by Förster resonance energy transfer. The binding sites of the chromen-4-one with bovine serum albumin are reported by molecular modeling.

1. Introduction

Albumins form drug–protein complexes and transport the drugs to their destination. Since serum albumins are present in much higher amounts in the blood than the other proteins, most of the studies focusing on protein–drug binding is centered on serum albumins. The fate of therapeutic drug molecules in the blood stream needs to be studied in detail in order to understand their pharmacological behavior [1]. The bio-distribution, and the elimination of drugs occurring in the body depends on the strength of the protein–drug binding [2,3]. Bovine serum albumin (BSA) is a model protein used for studying the serum protein binding of drugs [4]. It is mostly identical to human serum albumin in its sequence of amino acids. About 52–62% of the total plasma protein fraction are represented by BSA [5]. There are three domains in BSA viz., I, II, and III domains and these in turn contain sub-domains [6,7]. Trp-134 and Trp-212 are the tryptophans present in BSA, with Trp-134 the sub-domain IB [7–9].

β-Cyclodextrin is a cyclic doughnut shaped compound having seven D-glucopyranose units [10–12]. This molecule has a hollow center which can accommodate a variety of drug molecules based on their size and hydrophobicity. The complexes formed by β-cyclodextrin can enhance the solubility and stability of drugs in water [13–16] and increase their bio-availability [17,18].

We consider such an investigation substantial due to the following reasons: (i) gathering information on whether cyclodextrin complexation increases or decreases the strength of binding of drugs with carrier proteins can help understanding the release rate of drugs, (ii) the idea of blocking a part of the small molecule can lead to better knowing the pharmacophore activity, and (iii) the mechanism of action of specific pro-drugs can be exactly known by blocking their cleavage by cyclodextrins and studying their pharmacokinetics. Our lab has been active in this area of research since the work hinges on the rationale of novel sustained release of drugs from carrier molecules and the tuning of drug binding to macromolecular targets [19–21].

Coumarins form a structural part of many drugs. After oral administration coumarin is absorbed and metabolized, only 2 to 6% of it reaches the systemic circulation [22]. Due to the importance of coumarin in its *in-vivo* action, it has now been accepted as a pro-drug. About 35% of coumarins and 47% of 7-hydroxycoumarins bind to plasma proteins [23]. Pertaining to the pharmacological significance of aminocoumarin derivatives, we synthesized a new coumarin Schiff's base, 6-methyl-3-phenyliminomethyl-4H-chromen-4-one (MPIMC). In host-guest complexes, the part of guest molecules which remain outside the cyclodextrin cavity can bind to bio-macromolecules. Encapsulation by CD can tune the binding of small molecules with DNA [24–26]. However, studies on the binding of organic molecules in cyclodextrin–encapsulated form with protein are scarce [27]. In this paper, we extend insight into the Schiff's base's encapsulation by β-cyclodextrin (β-CD) and the binding of the compound in free and β-CD–encapsulated forms with BSA.

* Corresponding author.
E-mail address: drisraelenoch@gmail.com (E. Israel V.M.V.).

http://dx.doi.org/10.1016/j.molliq.2016.07.056
0167-7322/

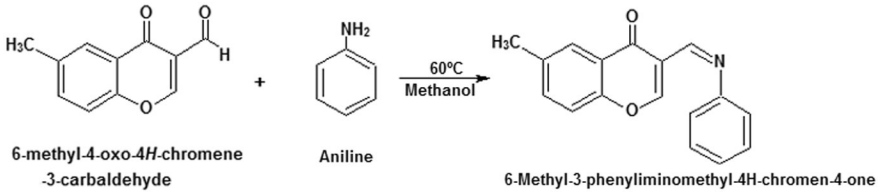

Fig. 1. The reaction scheme for the synthesis of MPIMC.

The binding strengths of MPIMC and MPIMC/β-CD with BSA are calculated using fluorescence spectroscopic studies. The resonance energy transfer (FRET) efficiencies between the BSA and MPIMC in water and in aqueous β-CD solution are explained.

2. Experimental

2.1. Chemicals

Sigma–Aldrich product of 6-methyl-3-formylchromone (AR) was purchased from Bangalore. Aniline (AR) was obtained from Merck, India and used as such without further purification. Solutions of various pH were made with phosphate buffer mixing phosphoric acid and sodium hydroxide (Qualigens). A modified Hammett's acidity scale [28] is used for the measurement of H_0 and pH value below the pH 2. Crystalline bovine serum albumin, HEPES buffer and β-cyclodextrin were purchased from Hi Media. All the solvents (products of Merck) were of spectral grade and used as received.

2.2. Synthesis and characterization of MPIMC

6-Methyl-3-phenyliminomethyl-4H-chromen-4-one was synthesized as per the reported procedure [29] and the reaction scheme is given in Fig. 1. An equimolar (2.66 mmol) amount of 3-formyl-6-methylchromone (0.5 g) and aniline (0.25 g) were stirred with 50 ml of methanol. The mixture was heated to 60 °C for 0.5 h and cooled to room temperature. Pale yellow crystals were separated out. The completion of the reaction was monitored by TLC and purified by column chromatography using hexane:ethyl acetate mixture (80:20) as eluting solvent. The 1H and 13C-NMR spectra of MPIMC are shown in Figs. SI 1 and 2 respectively (in the supporting information). 1H-NMR (500 MHz, $CDCl_3$): Chemical shift, δ 2.342 (s, 6–CH_3), δ 11.897 (d, 2–CH), δ 13.755 (d, 11–CH), δ 7.111–8.998 (Aromatic protons). 13C-NMR (500 MHz, $CDCl_3$): Chemical shift, δ 20.32 (6–CH_3), δ 163.75 (2–C), δ 125.18 (3–C), δ 154.46 (11–C), δ 181.63 (4 C = O), δ 116.2–152.68 (Aromatic carbons).

2.3. Preparation of MPIMC/β-CD solid complex

In a 50 ml beaker, MPIMC (0.25 g, 0.95 mmol) was dissolved in 5 ml of methanol. 5 ml of aqueous β-CD (1.0 g, 0.95 mmol) was prepared in another 50 ml beaker separately. A solution of MPIMC was added slowly to the solution of β-CD at room temperature in an Ultra-sonicator and maintained for 30 min to get homogenous solution medium. Then the mixture was warmed to 50 °C for 10 min and kept at room temperature for two days. The solid obtained was re-crystallized and analyzed.

2.4. Preparation of test solutions

Test solutions were prepared by appropriate dilution of a stock solution of MPIMC. The stock solution of MPIMC was made with methanol due to its poor solubility of in water. The test solutions were having

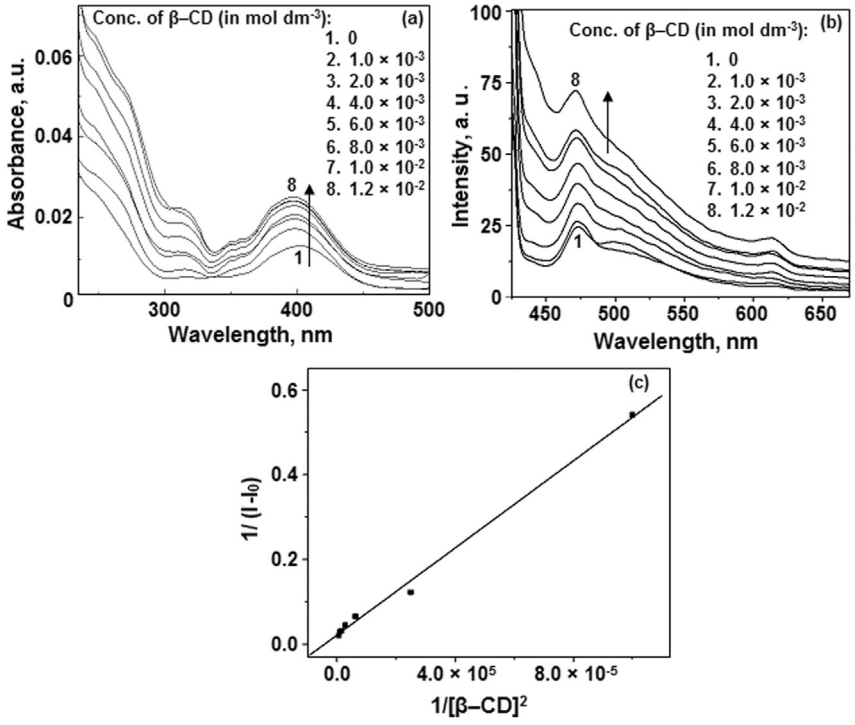

Fig. 2. (a). Absorption spectra of MPIMC in varying concentrations of β-CD (b). Fluorescence spectra of MPIMC in varying concentrations of β-CD (c). Benesi – Hildebrand plot of MPIMC/β-CD complex.

Table 1
Absorption and fluorescence spectral data of MPIMC in various concentrations of β-CD.

Conc. of β-CD, mol dm^{-3}	Absorption maximum, nm	Absorbance, a.u.	Fluorescence maximum, nm
0	403	0.0130	473.0
1.0×10^{-3}	398	0.0172	472.0
2.0×10^{-3}	398	0.0196	472.0
4.0×10^{-3}	398	0.0207	472.0
6.0×10^{-3}	398	0.0229	472.0
8.0×10^{-3}	398	0.0240	472.0
1.0×10^{-2}	397	0.0241	471.5
1.2×10^{-2}	397	0.0250	471.5

the concentration of methanol as 1% (*v*/*v*). HEPES buffer (0.1 M) is used to prepare stock solutions of the BSA of concentration 3.0×10^{-5} mol dm^{-3}. All reagents and solvents used were of spectral grade, which were used without further purification. Twice-distilled water was used throughout the experiments. All experiments were carried out at ambient temperature of 25 ± 2 °C. The test solutions were homogeneous after the addition of all additives. The absorption and the fluorescence spectra were recorded against appropriate blank solutions.

2.5. Instrumentation

Jasco V-630, double beam UV–Visible spectrophotometer was used for absorption measurements using 1 cm path length cells. A Perkin-Elmer LS55 spectrofluorimeter equipped with a 120 W Xenon lamp for excitation served the measurement of fluorescence. Both the excitation and the emission bandwidths were set up at 2.5 nm. Time–resolved fluorescence measurements were done on a time–correlated single photon counting (HORIBA) spectrofluorimeter. Ultra-sonicator (PCI 9 L 250H, India) was used for sonication. pH solutions were adjusted using an Elico LI 120 pH meter (India). 1H, 13C and two dimensional rotating frame Overhauser effect (ROESY) NMR spectroscopic technique were recorded on a Bruker AV III instrument operating at 500 MHz. $CDCl_3$ was used as the solvent for 1H and 13C-NMR spectra and DMSO–d_6 for MPIMC/β-CD complex in recording 2D ROESY NMR spectra. The internal standard was Tetramethylsilane (TMS) and the chemical shift values were obtained downfield from TMS in parts per million (ppm). The 2D ROESY experiments were performed using the prepared solid complex of MPIMC–β-CD. The mixing time for ROSEY spectra was 200 *ms* under the spin lock condition.

Molecular docking was done using a Schrodinger Maestro (Version 8.5) QSite QM/MM Program. The structure of BSA [PDB: 4F5S] was used from the Protein Data Bank database in which single sequence is used for the molecular docking studies. The structure of MPIMC was optimized to three dimensional orientations for the docking with the BSA. MPIMC was docked with the single sequence BSA by standard precision and extra precision methods. The best poses of the molecular docking for the binding of drug–BSA was considered from the Glide score (G-score) value [30]. G-score approximates a systematic search of active binding sites of the guest with the host binding site using a series of hierarchical filters [31].

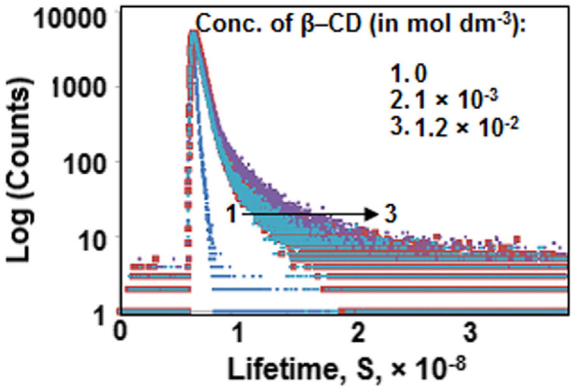

Fig. 3. Time–resolved fluorescence spectra of MPIMC.

3. Results and discussion

The absorption spectrum of MPIMC in water and in various amounts of the added aqueous β-CD solution is shown in Fig. 2 (a). Table 1 lists out the absorption spectral data. The absorption at 262 nm shows a small red shift with an increase in the concentration of β-CD is ascribed to the host-guest association of MPIMC in β-CD and due to the surfactant action of β-CD. Moreover, the absorbance continuously increases on each addition of β-CD up to a concentration of 1.2×10^{-2} mol dm^{-3} of β-CD. The fluorescence spectra of MPIMC with various amounts of β-CD are shown in Fig. 2 (b). An enhancement of fluorescence is observed at the addition of β-CD to MPIMC in water. The fluorescence band at 473 nm is shifted by 1.5 nm towards the blue (Table 2). Small blue shifts are generally indicative of non-bonded interactions and the dislodging of the guest molecule from the polar environment to the non-polar cavity of the cyclodextrin. If there had been any bond formations, there would have been large shifts of bands or formation of new bands. The stoichiometry and the association constant of the complex of MPIMC with β-CD was found out from the Benesi–Hildebrand equation [32] given as

$$\frac{1}{I-I_0} = \frac{1}{I'-I_0} + \frac{1}{I'-I_0}\frac{1}{K[\beta-CD]^2} \quad (1)$$

where I is the intensity at each concentration of β-CD, I_0 is the fluorescence intensity of MPIMC in water and I′ is the fluorescence intensity at the highest concentration of β-CD. K is the association constant and its value is calculated as 4.14×10^4 mol^{-2} dm^6. The linearity observed for the plot $1/(I\text{-}I_0)$ vs. $1/[\beta\text{-CD}]^2$ implies that the stoichiometry of the inclusion complex is 1:2 complexation is given in Fig. 2 (c).

The fluorescence decays of MPIMC–β-CD were recorded in aqueous medium at the same excitation and observation wavelengths. Fig. 3 shows the time–resolved fluorescence spectra of MPIMC in pure water and at low and high concentrations of β-CD. The fluorescence decay profile in water is bi-exponential with the relative amplitudes of 90.16 and 9.84 with the corresponding fluorescence lifetimes of 1.49 ns and 8.57 ns respectively. The decay profile becomes tri-exponential due to the new species formed i.e., β-CD complexed–MPIMC. This analysis

Table 2
Time–resolved fluorescence spectral data of MPIMC in water and β-CD.

Conc. of β-CD, mol dm^{-3}	Energy states	Lifetime (s)	Relative Amplitude (%)	χ2	Standard deviation (s)
0	T1	1.4857×10^{-9}	90.16	1.1247	4.7467×10^{-12}
	T2	8.5712×10^{-9}	9.84		1.0018×10^{-10}
1.0×10^{-3}	T1	7.2393×10^{-10}	18.79	1.1765	1.1204×10^{-10}
	T2	1.7424×10^{-9}	66.03		1.6942×10^{-11}
	T3	9.2534×10^{-9}	15.17		8.9920×10^{-11}
1.2×10^{-2}	T1	4.4244×10^{-10}	23.65	1.1242	2.7085×10^{-11}
	T2	1.5247×10^{-9}	66.25		1.2145×10^{-11}
	T3	7.8639×10^{-9}	10.10		9.7986×10^{-11}

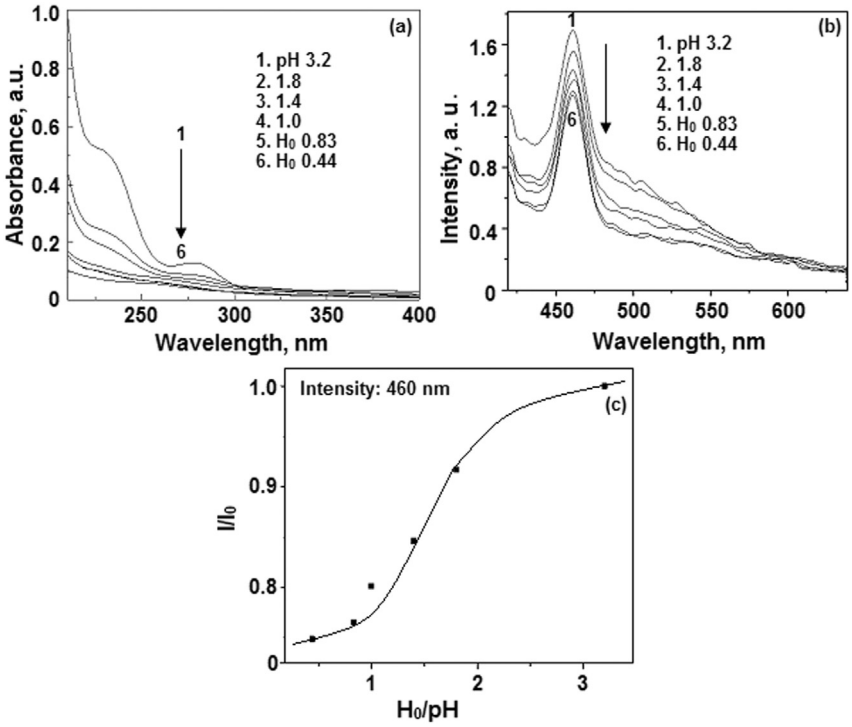

Fig. 4. (a) Absorption spectra of MPIMC at various pH in water (b) Fluorescence spectra of MPIMC at various pH in water (c) I/I_0 versus H_0/pH plot of MPIMC in water.

supports the view that two emitting individuals are present in solution possessing different fluorophore populations viz., the free and the β-CD–complexed form of MPIMC. The formation of a new species with a different lifetime is an evidence for the formation of the host–guest complex. The lifetime of this species increases in high concentration of β-CD whereas the status corresponding to the free MPIMC remains unmodulated between low and high concentrations of β-CD. These changes are related to the host–guest association between MPIMC and β-CD.

In order to add further evidence to the result that the complex formed between MPIMC and β-CD is host-guest complex and not any non-inclusional association, the absorption and the fluorescence spectra

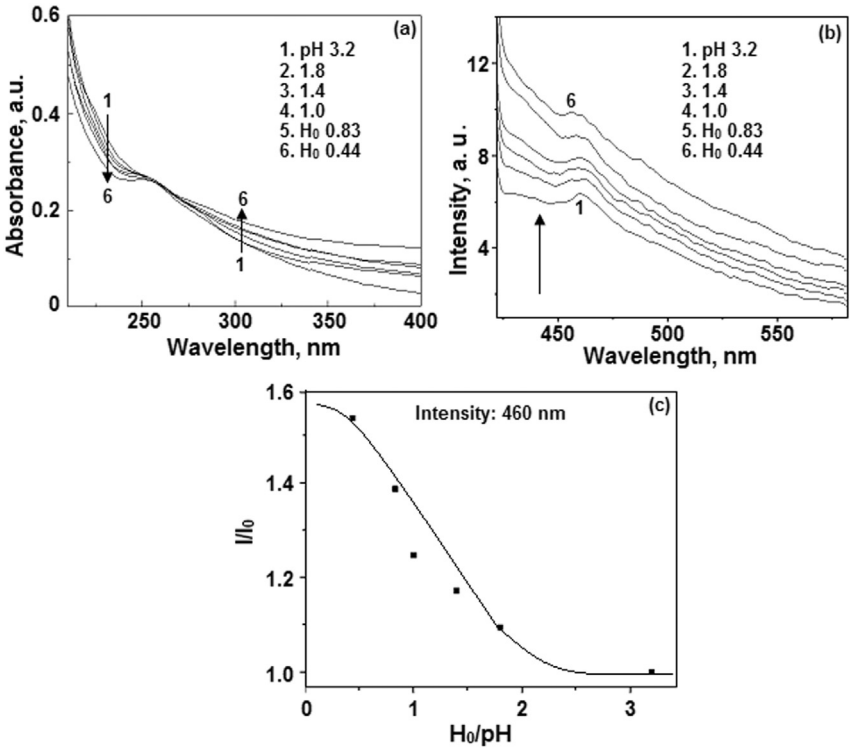

Fig. 5. (a) Absorption spectra of MPIMC at various pH in β-CD (b). Fluorescence spectra of MPIMC at various pH in β-CD (c). I/I_0 versus H_0/pH plot of MPIMC in β-CD.

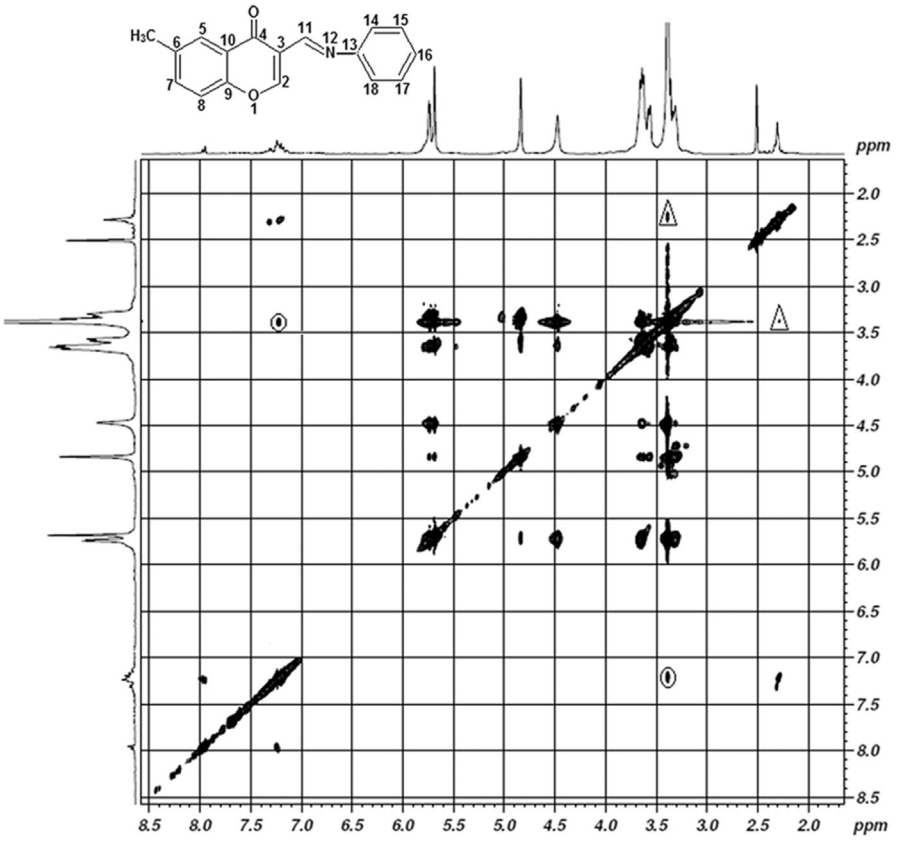

Fig. 6. 2D ROESY spectra of MPIMC-β-CD complex.

of MPIMC are recorded with various amounts of D-(+)-glucose. The fluorescence intensity is not significantly altered due to the addition of D-(+)-glucose. This suggests that the hydrophobic cavity of β-CD indeed plays a role in the changes observed in the spectra.

In order to find out low acidic strength affects the spectra of MPIMC with and without β-CD and to extend insights into the mode of binding of MPIMC with β-CD; we measured the absorption and fluorescence spectra at various H_0/pH in water and in β-CD. With the decrease of pH, the absorption band at 262 nm showed a decrease of absorbance in Fig. 4 (a) which indicates that equilibrium exists between the neutral and the cationic forms of MPIMC. The ground state pK_a value is calculated using the expression [33] (Eq. (4)) derived as follows:

$$C_1 = \frac{A(\lambda 1)\varepsilon 2(\lambda 2) - A(\lambda 2)\varepsilon 2(\lambda 1)}{\varepsilon 2(\lambda 1)\varepsilon 2(\lambda 2) - \varepsilon 1(\lambda 2)\varepsilon 2(\lambda 1)} \quad (2)$$

$$C_2 = C_T - C_1 \quad (3)$$

where C_T is the total concentration of the compound in both forms and $\varepsilon_1(\lambda_1), \varepsilon_2(\lambda_2), \varepsilon_2(\lambda_1), \varepsilon_2(\lambda_2)$ are the molar extinction coefficients of the protonated and neutral forms at wavelengths λ_1 (262 nm) and λ_2 (225 nm) respectively.

$$pK_a = pH + \log C_1/C_2 \quad (4)$$

The calculated ground state pK_a is 1.12. Decrease of pH shows a quenching of fluorescence as seen in Fig. 4 (b). This may be due to proton–induced fluorescence quenching. However, a new band in the protonated form of MPIMC could not be found and hence the excited state pK_a cannot be calculated. Fig. 4 (c).

The effect of acidity on the absorption and fluorescence of MPIMC in the presence of β-CD are shown in Fig. 5 (a) and (b) respectively. There is an isosbestic point at 270 nm in the absorption spectra indicating the existence of equilibrium between the free and the protonated forms of the MPIMC molecule. The ground state pK_a calculated is 0.98. Quite contrary to the effect of acidity on MPIMC in water, at the addition of β-CD, the fluorescence gets quenched on increase of acid strength. This may be due to some phenomenon other than collisional quenching. This occurs due to the inaccessibility of the guest molecule being encapsulated strongly by two β-CD molecules. The change in the relative intensity of fluorescence with pH is shown in Fig. 5 (c).

In order to confirm 1:2 stoichiometry of the MPIMC/β-CD complex and to optimize the structure of the inclusion complex, 2D ROESY spectrum was recorded (Fig. 6). Cross correlation peaks are observed between the signals of methyl protons in the positions of 6 of MPIMC and H4 protons of β-CD (marked with a triangle). This reveals that the methyl group of MPIMC is surrounded by one β-CD molecule. The aromatic protons of imine-linked phenyl ring interact with the H4 proton of β-CD which is due to the engulfing of phenyl ring to the hydrophobic cavity of another β-CD. This occurs due to the free availability of the phenyl ring. This cross peak is marked with a circle in Fig. 6. Here we could not observe the correlation peak between the protons of another β-CD molecule and the aromatic protons of the chromone moiety in MPIMC. This may be to the steric hindrance offered by chromone ring

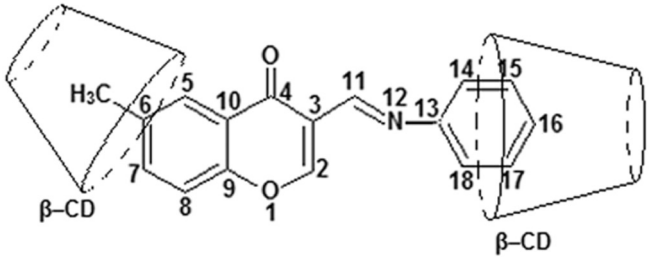

Fig. 7. Structural representation of 1:2 stoichimetry complex of MPIMC-β-CD.

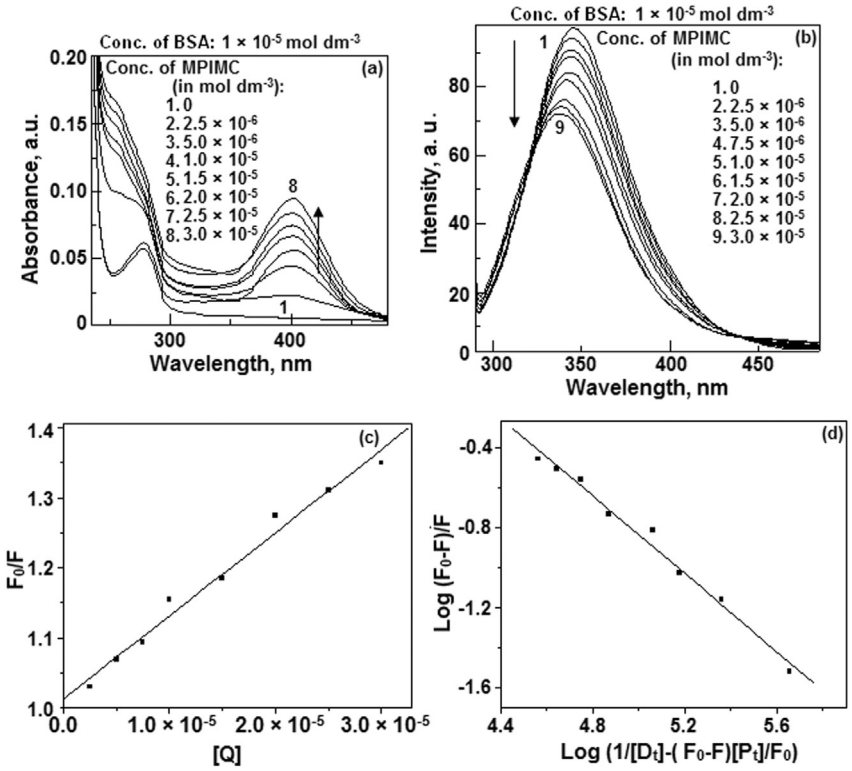

Fig. 8. (a) Absorption spectra of BSA with various concentrations of MPIMC (b). Quenching of tryptophan fluorescence of BSA due to binding with MPIMC (c). The Stern–Volmer quenching plot of BSA by MPIMC (d). The plot of log $(1/[D_t] - (F_0\text{-}F)[P_t]/F_0)$ versus log $(F_0\text{-}F)/F$ for the binding of MPIMC with BSA.

in covering the aromatic group by β-CD. The cross peak observed for the methyl protons in position 6 is due to the partial coverage of β-CD. Based on the above arguments, the 1:2 inclusion complex of MPIMC withβ-CD could have the structure as given in Fig. 7.

The binding titration of MPIMC with bovine serum albumin was carried out with a constant concentration of BSA kept at 3.0×10^{-5} mol/dm^3 and adding aliquots of MPIMC [Fig. 8 (a)]. At the maximal concentration of MPIMC there were 0.3 absorbance units (more than 0.1) both at 400 nm (absorption maximum) and at 473 nm (fluorescence maximum). Therefore the inner filter effect was corrected before further experiments. The inner filter effect was nullified with a correction of fluorescence intensity by including a correction factor from the equation [34] which considers re-absorption of the emitted photons.

$$F_{cor} = F_{obs} \times e^{(Aex+Aem)/2} \quad (5)$$

where F_{cor} is the corrected fluorescence intensity and F_{obs} is the observed intensity of fluorescence, A_{ex} is the absorbance at excitation wavelength and A_{em} is that at the emission wavelength.

The absorption band at 265 nm is distinctly seen in water, but it disappears at the addition of BSA with the band shifting to the blue continuously. The shoulder at the shorter wavelength on complete binding of MPIMC with BSA is centered at 255 nm which is a large shift from 265 nm. The absorbance continuously increased with the addition of BSA. The longer wavelength band observed at 403 nm is bathochromically shifted only by 2 nm. These results are due to the highly hydrophobic environment offered by the BSA macromolecule for MPIMC.

The quenching of tryptophan fluorescence of BSA by MPIMC is shown in Fig. 8 (b). The fluorescence quenching is linear which is attributed to the binding of MPIMC with BSA. There is no other process except

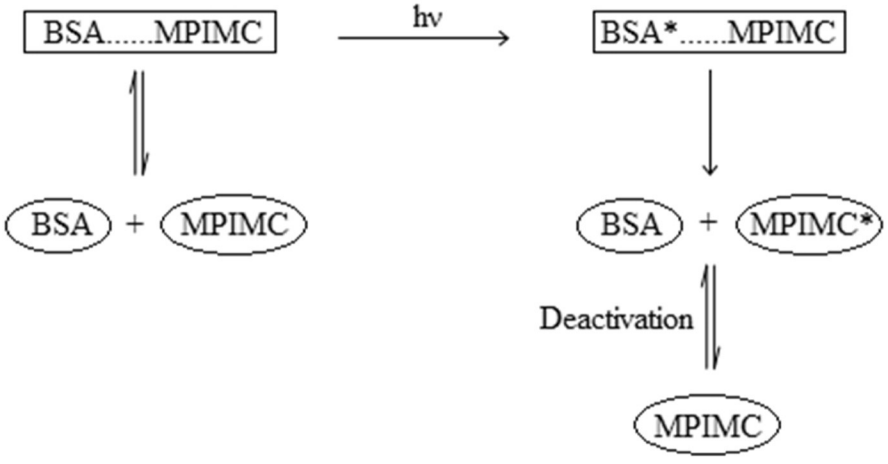

Scheme 1. Energy transfer between BSA and MPIMC.

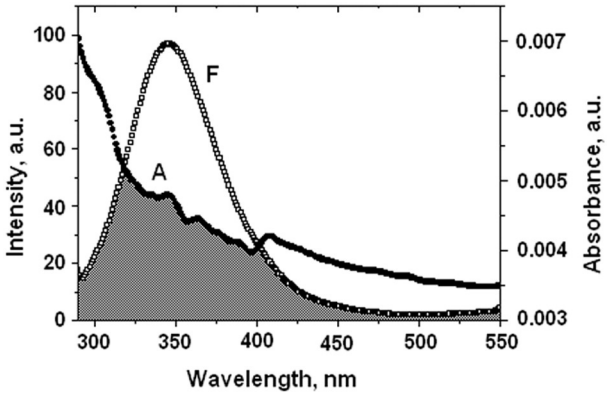

Fig. 9. The spectral overlap of the absorption spectrum of MPIMC (A) and the fluorescence emission spectrum of BSA (F).

binding of these two. The fluorescence spectrum shows a blue shift of 8 nm due to the non-polar environment offered by the BSA molecule. Fluorescence quenching is well known to be classified into dynamic and static types. The quenching mechanism between MPIMC and BSA was analyzed using the titration data, applying the Stern–Volmer equation (Eq. (6))

$$\frac{F_0}{F} = 1 + K_q\ \tau_0[Q] = 1 + K_{SV}[Q] \tag{6}$$

where F_0 and F are the fluorescence intensities of BSA without and with the quencher respectively. K_q is the bimolecular quenching rate constant and τ_0 is the lifetime of the BSA in water. [Q] is the quencher concentration and K_{SV} is the Stern–Volmer quenching constant. The Stern–Volmer plot for the quenching of fluorescence by MPIMC is shown in Fig. 8 (c). The calculated K_{SV} is $1.18 \times 10^4\ mol^{-1}\ dm^3$.

The apparent association constant for the binding of MPIMC with BSA the stoichiometry of the binding is calculated from the plot [Fig. 8 (d)] of $\log\{1/[D_t]\text{-}(F_0\text{-}F)[P_t]/F_0\}$ vs. $\log(F_0\text{-}F)$ following Eq. (7).

$$\log_{10}\left(\frac{F_0 - F}{F}\right) = n\log_{10}K_A - n\log_{10}\left(\frac{1}{[D_t] - (F_0 - F)[P_t]/F_0}\right) \tag{7}$$

In this equation, F_0 and F are the fluorescence intensities without and with the quencher respectively, $[D_t]$ is the total quencher concentration and $[P_t]$ is the total protein concentration [35]. The association constant (K) is calculated to be $1.37 \times 10^4\ mol^{-1}\ dm^3$ and the stoichiometry is ≈ 1.

Forster's non-radiative energy transfer theory aids the estimation of the distance between the buried BSA and the bound MPIMC.

There can be an energy transfer between the tryptophan residues of BSA and the bound MPIMC with the BSA acting as donor and the MPIMC as acceptor [Scheme 1]. The overlap of the fluorescence spectrum of BSA and the absorption spectrum of MPIMC is shown in Fig. 9. The efficiency of energy transfer (E), the donor – acceptor binding distance and the critical distance (R_0) are calculated [36] using the following Eqs. (8) to (10),

$$E = 1 - F/F_0 = R_0^6 + r_0^6 \tag{8}$$

where R_0 is the Förster distance at 50% energy transfer and r_0 is the distance between the donor and the acceptor. R_0 is calculated as follows,

$$R_0^6 = 8.8 \times 10^{-25}\left[\kappa^2 n^{-4} \Phi_D J(\lambda)\right] \text{in } Å^6 \tag{9}$$

where n is the refractive index of the medium, ϕ_D is the relative interaction with acceptor, κ^2 is the relative orientation of the donor and

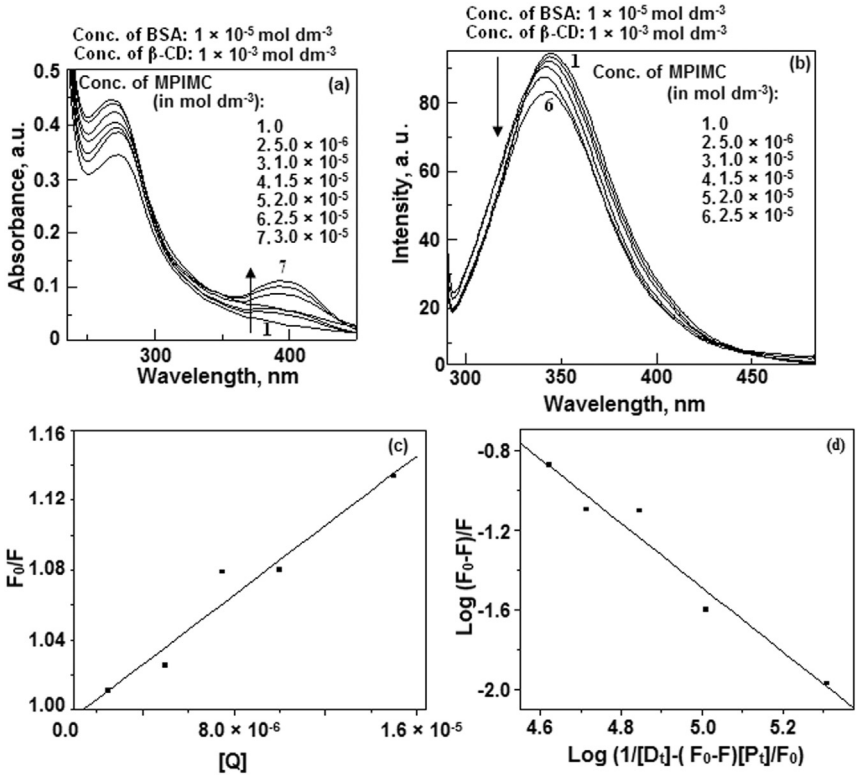

Fig. 10. (a). Absorption spectra of BSA with various concentrations of MPIMC-β-CD complex (b). Quenching of tryptophan fluorescence of BSA due to binding with MPIMC-β-CD complex (c). The Stern–Volmer quenching plot of BSA by MPIMC-β-CD complex (d). The plot of log $(1/[D_t] - (F_0\text{-}F)[P_t]/F_0)$ versus log $(F_0\text{-}F)/F$ for the binding of MPIMC-β-CD complex with BSA.

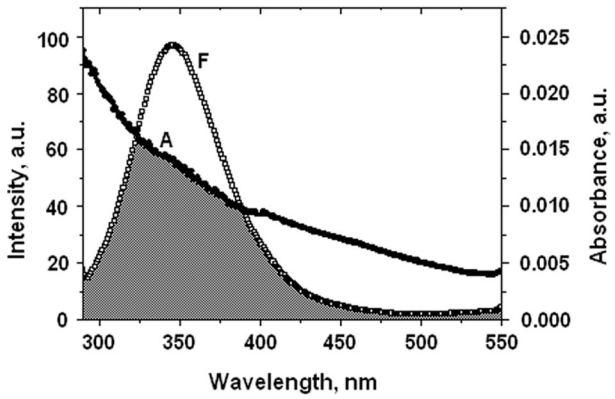

Fig. 11. The spectral overlap of the absorption spectrum of MPIMC-β-CD (A) and the fluorescence emission spectrum of BSA (F).

acceptor, and J(λ) is the overlap integral of the absorption spectrum of the acceptor and the fluorescence spectrum of the donor. J(λ), the overlap integral is given by

$$J = \frac{\int_0^{\infty} F_D(\lambda)\varepsilon_A(\lambda_0)\lambda^4 d\lambda}{\int_0^{\infty} F_D(\lambda)d\lambda} \quad (10)$$

In the above equation $F_D(\lambda)$ refers to the corrected fluorescence intensity of the donor between the wavelengths λ and (λ + Δλ), and ε_A (λ) is the molar extinction coefficient of the acceptor at the wavelength λ. Random orientations of the donor and the acceptor are assumed. The results obtained are $n = 1.33$, $J = 7.39 \times 10^{-21}$ M^{-1} cm^{-1} nm^4, E = 0.029, $R_0 = 2.433$ nm, and $r_0 = 4.354$ nm. The donor–to–acceptor distance (4.354 nm) confirms that static quenching occurs with the energy transfer from BSA to MPIMC.

According to the literature, there is almost no influence of β-CD on BSA [37]. The absorption spectrum of MPIMC–β-CD complex with various amounts of BSA is shown in Fig. 10 (a). The blue shift of absorbance is less compared to the shift in water. This is due to the protonated environment offered by β-CD to MPIMC from BSA. However, the absorbance increases, which indicate that binding with BSA occurs. Fig. 10 (b) shows the quenching of tryptophan fluorescence of BSA due to binding with MPIMC. There is an isosbestic point due to the equilibrium between MPIMC–β-CD and its complex with BSA. The quenching magnitude in the presence of β-CD is lesser compared to that in water. The Stern–Volmer quenching plot for the above mentioned interaction is shown in Fig. 10 (c). The calculated Stern–Volmer constant is 9.94×10^3 mol^{-1} dm^3. This is lesser when compared the case of binding of MPIMC with BSA in water. The plot of log (1/[Dt] – (F_0-F)[Pt]/F_0) vs. log (F_0-F)/F for the binding of MPIMC-β-CD with BSA following Eq. (5) is shown in Fig. 10 (d). The association constant is determined as 1.18×10^3 mol^{-1} dm^3. The association constant value is smaller than that for the binding of free MPIMC with BSA (in water). Hence cyclodextrin complexation decreases the strength of binding of the MPIMC molecule with BSA, due to the reason that MPIMC is covered up by β-CD from the approach of BSA molecule for binding. This observation leads to the idea that cyclodextrin encapsulation can help the transport of drugs in blood stream by binding with the BSA and the bound drug is more readily released than the free drug stronger bound with BSA.

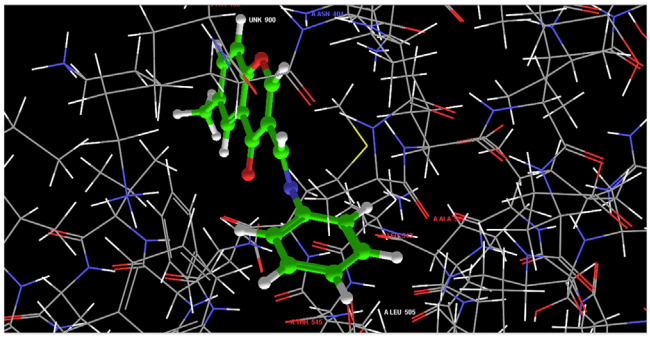

Fig. 12. Molecular docking poses of MPIMC with BSA.

Fig. 11 shows the overlap of the fluorescence spectrum of BSA with the absorption spectrum of MPIMC-β-CD complex. The calculated values of n, Φ, J, E, R_0, and r_0 are 1.33, 0.15, 2.01×10^{-21} M^{-1} cm^{-1} nm^4, 0.010, 2.875 nm and 6.115 nm, respectively with the method discussed earlier in the case of MPIMC–BSA binding. These values are different from the values obtained for MPIMC binding with BSA in water. Hence cyclodextrin clearly modulates the binding.

Further insight into the mode of MPIMC–BSA binding was offered by molecular modeling. BSA consists the major domains I, II, and III with the residues 1–183 in domain I, 184–376 in domain II, and 377–583 in domain III. The hydrophobic cavity in sub-domain IIA can allow the drug molecule to get accommodated, which plays a vital role in the transportation of drugs in BSA. The best energy ranked results (Fig. 12) reveal that MPIMC is located within the sub-domain III hydrophobic cavity in close proximity to the residues, such as Leu-505, Ala-527, Leu-543, and Thr-545 suggesting that there occurs a hydrophobic contribution to the binding. Moreover, hydrogen bonding is revealed at these sites. Hence, this finding explains the effective quenching of fluorescence of BSA by MPIMC. Furthermore, there are many of hydrophobic interactions; many several apolar residues close to the ligand aid in stabilizing the molecule via phobic interactions. The hydrogen bonds increase the stability of the MPIMC–BSA bound system. Therefore, the interaction between the MPIMC and BSA is dominated both by hydrophobic binding and hydrogen bonds. Since β-CD blocks some of the possible hydrogen bond formation between MPIMC and BSA, the binding strength of MPIMC–β-CD with BSA is relatively low compared to that of MPIMC in water.

4. Conclusions

MPIMC forms 1:2 inclusion complex with β-CD and the association constant is determined as 4.14×10^4 mol^{-2} dm^6. This is evidenced by fluorescence spectroscopy and 2D ROESY correlation spectroscopy. The decrease of pK_a for the equilibrium of MPIMC in the presence of β-CD than in water, revealing the restriction to protonation offered by the β-CD. Study of the binding of MPIMC with BSA is carried out in the absence and the presence of β-CD. The calculated K_{SV} for the quenching of fluorescence of BSA by MPIMC is 1.18×10^4 mol^{-1} dm^3. The association constant is calculated as 1.37×10^4 mol^{-1} dm^3 and the stoichiometry is 1. In the presence of β-CD the association constant is determined as 1.18×10^3 mol^{-1} dm^3. Förster resonance energy transfer between BSA and MPIMC is studied in the absence and the presence of β-CD. The donor–to–acceptor distance confirms that static quenching occurs with the energy transfer from BSA to MPIMC. This distance is smaller in the case of free MPIMC than the β-CD-complexed form of MPIMC binding with BSA. Hence the encapsulation by cyclodextrin decreases the strength of binding of the MPIMC molecule with BSA. Molecular modeling reveals that the binding of MPIMC through the hydrophobic and the hydrogen bonding sites of BSA. The hydrogen bonds increase the stability of the MPIMC–BSA bound system. Since β-CD blocks some of the possible hydrogen bonding sites between MPIMC and BSA, the binding strength of MPIMC–β-CD complex with BSA is relatively low with that of free MPIMC.

The Supplementary Material contains the 1H and 13C NMR spectrum for the synthesized MPIMC. Supplementary data associated with this article can be found in the online version, at http://dx.doi.org/10.1016/j.molliq.2016.07.056.

Acknowledgement

This work is financially supported by the Department of Science and Technology (DST), Government of India (Project file: SR/FT/CS-062/2009). We express our sense of gratitude to the DST. We extend our thanks to SAIF, Indian Institute of Technology–Madras, Chennai, for their help in NMR measurements.

References

[1] V.N. Uversky, N.V. Narizhneva, T.V. Ivanova, A.Y. Tomashevskis, Biochemistry 36 (1997) 13638.
[2] V.S. Jisha, K.T. Arun, M. Hariharan, D. Ramaiah, J. Am. Chem. Soc. 128 (2006) 6024.
[3] C.H. Yu, A. Al-Saadi, S.J. Shih, L. Qiu, K.Y. Tam, S.C. Tsang, J. Phys. Chem. C 113 (2009) 537.
[4] X.–.L. Han, F.–.F. Tian, Y.–.S. Ge, F.–.L. Jiang, L. Lai, D.–.W. Li, Q.–.L. Yu, J. Wang, C. Lin, Y. Liu, J. Photochem. Photobiol. B Biol. 109 (2012) 1.
[5] S. Nafisi, G.B. Sadeghi, A.P. Yab, J. Photochem. Photobiol. B Biol. 105 (2011) 198.
[6] M. Labieniec, T. Gabryelak, J. Photochem. Photobiol. B Biol. 82 (2006) 72.
[7] Y.–.J. Hu, H.–.L. Yue, X.–.L. Li, S.–.S. Zhang, E. Tang, L.–.P. Zhang, J. Photochem. Photobiol. B Biol. 112 (2012) 16.
[8] C.D. Kanakis, P.A. Tarantilis, M.G. Polissiou, S. Diamantoglou, H.A. Tajmir-Riahi, J. Mol. Struct. 798 (2006) 69.
[9] J.H. Tang, F. Luan, X.G. Chen, Bioorg. Med. Chem. 14 (2006) 3210.
[10] M. Valero, C. Carrillo, J. Photochem. Photobiol. B Biol. 74 (2004) 151.
[11] G. Zhang, S. Shuang, C. Dong, D. Liu, M.M.F. Choi, J. Photochem. Photobiol. B Biol. 74 (2004) 127.
[12] J. Szejtli, Cyclodextrin Technology, Kluwer Academic publishers, Dordrecht, 1988.
[13] M. Christoff, L.T. Okano, C. Bohne, J. Photochem. Photobiol., A 134 (2000) 169.
[14] M.E. Davis, M.E. Brewster, Nat. Rev. Drug Discov. 3 (2004) 1023.
[15] J. Jang, T.L. Yaksh, H.F. Hill, J. Pharmacol. Exp. Ther. 261 (1992) 592.
[16] T.X. Loftsson, M.E. Brewster, J. Pharm. Sci. 85 (1996) 1017.
[17] T. Srichana, R. Suedee, W. Reanmongkol, Respir. Med. 95 (2001) 513.
[18] M. Skiba, F. Bounoure, C. Barbot, P. Arnaud, M. Skiba, J. Pharm. Pharm. Sci. 8 (2005) 409.
[19] N. Sudha, Y. Sameena, I.V.M.V. Enoch, J. Solut. Chem. 45 (2016) 431.
[20] N. Sudha, I.V.M.V. Enoch, J. Solut. Chem. 44 (2015) 1367.
[21] N. Sudha, Y. Sameena, S. Chandrasekaran, I.V.M.V. Enoch, D. Premnath, Spectrosc. Lett. 48 (2015) 112.
[22] B. Lake, Food Chem. Toxicol. 37 (1999) 423.
[23] W.A. Ritschel, K.W. Grummich, S. Kaul, T.J. Hardt, Pharm. Ind. 43 (1981) 271.
[24] S. Yousuf, N. Sudha, G. Murugesan, I.V.M.V. Enoch, Carbohydr. Res. 365 (2013) 46.
[25] Y. Sameena, I.V.M.V. Enoch, J. Lumin. 138 (2013) 105.
[26] S. Yousuf, D. Radhika, I.V.M.V. Enoch, M. Easwaran, Spectrochim. Acta A 98 (2012) 405.
[27] N. Sudha, I.V.M.V. Enoch, J. Solut. Chem. 40 (2011) 1755.
[28] M.J. Jorgenson, D.R. Hartter, J. Am. Chem. Soc. 85 (1963) 878.
[29] K.M. Khan, N. Ambreen, S. Hussain, S. Perveen, M.I. Choudhary, Bioorg. Med. Chem. 17 (2009) 2983.
[30] Available online at www.schrodinger.com/docs/2003_1/pdf/firstdiscovery/fd27_technical_notes.pdf.
[31] E. Perola, W.P. Walters, P.S. Charifson, Proteins: Struct., Funct., Bioinf. 56 (2004) 235–249.
[32] I.V.M.V. Enoch, M. Swaminathan, J. Fluoresc. 16 (2006) 501.
[33] S. Chandrasekaran, I.V.M.V. Enoch, J. Spectro., Volume 2013, (Article ID 408506, 13 pages).
[34] V.W. Marco, S. Lorenzo, J. Mol. Struct. 998 (2011) 144.
[35] R. Liu, J. Yang, C.–.E. Ha, N.V. Bhagavan, R.G. Eckenhoff, Biochem. J. 388 (2005) 39.
[36] V.D. Suryawanshi, P.V. Anbhule, A.H. Gore, S.R. Patil, G.B. Kolekar, J. Photochem. Photobiol. B Biol. 118 (2013) 1.
[37] H.–.X. Zhang, X. Huang, M. Zhang, J. Fluoresc. 18 (2008) 753.